JOURNAL OF THE AMERICAN CHEMICAL SOCIETY

pubs.acs.org/JACS

Communication

Superatom Regiochemistry Dictates the Assembly and Surface Reactivity of a Two-Dimensional Material

Amymarie K. Bartholomew, Elena Meirzadeh, Ilana B. Stone, Christie S. Koay, Colin Nuckolls, Michael L. Steigerwald, Andrew C. Crowther, and Xavier Roy*

Cite This: J. Am. Chem. Soc. 2022, 144, 1119−1124

Read Online

ACCESS | Metrics & More | Article Recommendations | Supporting Information

ABSTRACT: The area of two-dimensional (2D) materials research would benefit greatly from the development of synthetically tunable van der Waals (vdW) materials. While the bottom-up synthesis of 2D frameworks from nanoscale building blocks holds great promise in this quest, there are many remaining hurdles, including the design of building blocks that reliably produce 2D lattices and the growth of macroscopic crystals that can be exfoliated to produce 2D materials. Here we report the regioselective synthesis of the cluster [*trans*-$Co_6Se_8(CN)_4(CO)_2]^{3-/4-}$, a "superatomic" building block designed to polymerize and assemble into a 2D cyanometalate lattice whose surfaces are chemically addressable. The resulting vdW material, $[Co(py)_4]_2$[*trans*-$Co_6Se_8(CN)_4(CO)_2$], grows as bulk single crystals that can be mechanically exfoliated to produce flakes as thin as bilayers, with photolabile CO ligands on the exfoliated surface. As a proof of concept, we show that these surface CO ligands can be replaced by 4-isocyanoazobenzene under blue light irradiation. This work demonstrates that the bottom-up assembly of layered vdW materials from superatoms is a promising and versatile approach to create 2D materials with tunable physical and chemical properties.

The breadth of 2D materials is constantly expanding,[1,2] yet there exist few exfoliatable van der Waals (vdW) materials whose structures can be modified in a predictable manner. vdW materials are typically obtained as large single crystals composed of just a few elements[3] and are difficult to synthetically modify without completely changing their compositions or structures.[4−6] 2D metal−organic frameworks and covalent organic frameworks offer synthetic flexibility, but large single crystals are rare, preventing their exfoliation and study at the 2D limit.[7,8] Without synthetically tunable vdW materials, we cannot study properties as a function of programmatic changes to the 2D system. Manipulation of the surface chemistry of ultrathin materials is particularly desirable, as this can change their height, doping level, reactivity, photophysics, and interactions in heterostructures.[9−11] This presents an opportunity for synthetic chemists—can we create exfoliatable 2D materials whose properties can be tuned through synthetic manipulations?

Atomically precise molecular clusters (so-called "superatoms") are promising building blocks for synthetically tunable 2D materials.[12−17] Superatomic properties depend on the cluster core, ligand periphery and oxidation state,[18] and superatoms can be assembled into ionic materials via charge transfer[15,19,20] and into frameworks via cluster fusion[21] or through molecular bridges.[14,22−32] Cyanides are especially attractive bridges as they enable strong mechanical, electronic, and magnetic coupling between a variety of metals.[33−35] Octahedral clusters of the form M_6E_8 (M = transition metal, E = chalcogen) with six surface-capping cyanides have been polymerized into Prussian Blue-type structures with various metal ions, but the resulting structures are typically 3D cubic frameworks (Figure 1).[23−28,36,37]

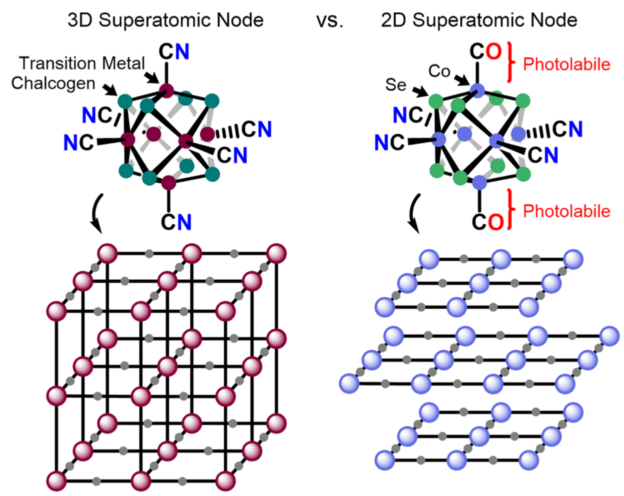

Figure 1. Superatomic building blocks for 3D and 2D lattices.

In this work, we detail a synthetic strategy to control the dimensionality of the framework using a site-differentiated superatom with four cyanides around its belt and two carbonyls at the apexes (Figure 1). The two groups have orthogonal reactivity: the cyanides can bridge but are inert toward substitution while the carbonyls are photolabile but do

Received: November 15, 2021
Published: January 12, 2022

https://doi.org/10.1021/jacs.1c12072
J. Am. Chem. Soc. 2022, 144, 1119−1124

not bridge. We find the "2D superatomic node" [*trans*-$Co_6Se_8(CN)_4(CO)_2]^{3-}$ (**1**) forms a layered vdW material that can be mechanically exfoliated to produce atomically thin flakes whose surfaces can be functionalized through simple photoinduced substitution chemistry. The structure presented herein can be described as a cyanometalate form of a dimensionally reduced perovskite lattice,[38] making it one of only a handful of known Lieb lattices—a desirable depleted square lattice whose unique topology can give rise to nontrivial flat bands, superconductivity, and the fractional quantum Hall effect.[39−42]

We grow single crystals of the vdW material $[Co(py)_4]_2$[*trans*-$Co_6Se_8(CN)_4(CO)_2$] (**2**) by layering an aqueous solution of cobalt dibromide ($CoBr_2$) on top of 1equiv of **1** and pyridine (py) in water. The layers mix to form a fine suspension, from which flat, square crystals of **2** grow over 7 days. Single crystal X-ray diffraction (SCXRD) reveals **2** is a square 2D lattice of *trans*-$Co_6Se_8(CN)_4(CO)_2$ linked by $Co(py)_4$ sites (Figure 2a). Each 2D layer is porous, with disordered water molecules occupying the pores, but the material lacks accessible porosity because ABAB packing along the *c*-direction positions superatoms from one layer directly over the pores of its neighboring layers (Figure 2b).

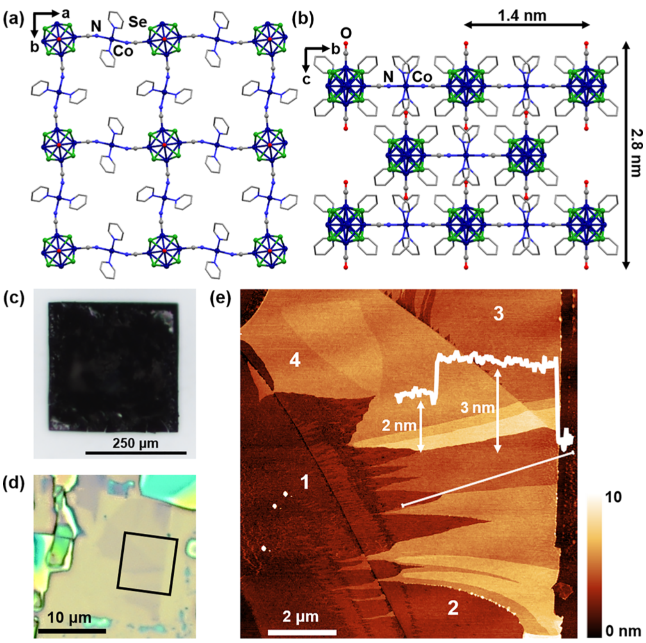

Figure 2. (a, b) Crystal structure of $[Co(py)_4]_2$[*trans*-$Co_6Se_8(CN)_4(CO)_2$] (**2**) showing a top view of a single layer (a) and a side view of the stacking along the *c*-direction (b). (c) Optical microscopy image of a crystal of **2**. (d) Optical microscopy image of an exfoliated flake of **2** on a Si/SiO_2 wafer. (e) AFM image and height profile (along the white line) of a thin flake of **2**. The number of layers is indicated on the regions of the flake. The black box in (d) denotes the area imaged in (e).

The 2:1 ratio of bridging Co sites to superatoms in **2** indicates that the superatom is reduced *in situ* to the 4^- state. Energy dispersive X-ray spectroscopy (EDS) of the crystals gives a 1:1 Co:Se ratio and confirms that there is no Br^- or other counterion in the lattice. Our assignment of the superatoms as 4^- and bridging $Co(py)_4$ as 2^+ is further supported by the SCXRD bond metrics, which are consistent with high-spin Co(II),[43] and the magnetic susceptibility data for **2**, which shows the expected ground state value of χT for two uncoupled $S = 3/2$ Co(II) sites and a diamagnetic superatom (Figures S11 and S12).

The crystal structure of **2** features layers with strong in-plane bonds and weak out-of-plane vdW interactions. By analogy to traditional atomic vdW materials, crystals of **2** (Figure 2c) can be mechanically exfoliated to produce atomically thin flakes (Figure 2d). Atomic force microscopy (AFM) shows these flakes have atomically flat surfaces (Figure 2e). We can reliably produce micrometer-size flakes as thin as 2 nm as determined by AFM, corresponding to a bilayer. Monolayers are also observed but tend to be rough, likely due to low mechanical stability of the porous Lieb lattice.

The key feature of this new 2D material is that its surfaces are passivated with photolabile CO ligands offering unique possibilities for surface functionalization. The photoinduced exchange of CO for phosphines and isocyanides on Co_6Se_8 clusters has been demonstrated in solution[44−46] but not in the solid state. As a first demonstration, we functionalize exfoliated flakes of **2** with 4-isocyanoazobenzene (CNAB), which allows us to monitor the reaction by Raman spectroscopy. Neither the carbonyl in **2** nor the isocyano group of CNAB, when bound to the superatom, are detectable by Raman spectroscopy because they lie perpendicular to the substrate (parallel to the incident laser). However, spectroscopic signatures from the azobenzene, including the N═N stretch, and from the cyanide ligands in the plane of the sheets are detectable by Raman spectroscopy (Figure 3).

To functionalize the exposed surfaces of the sheets, flakes of **2** exfoliated onto a Si/SiO_2 substrate are immersed in a

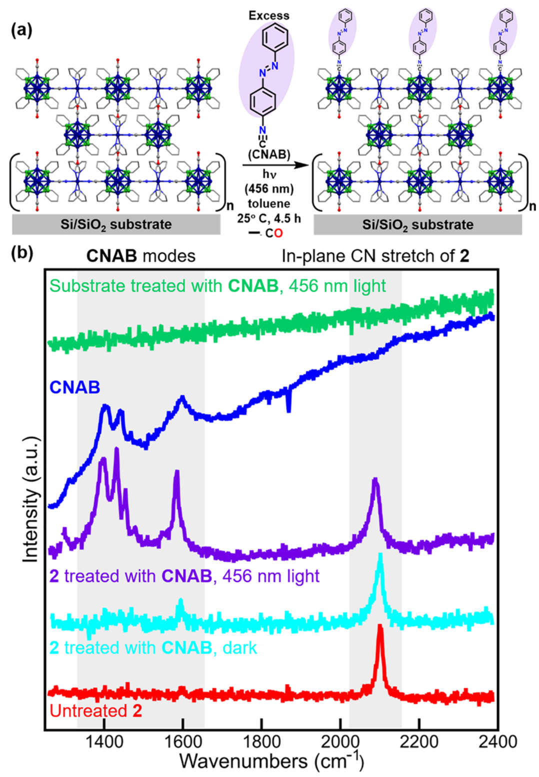

Figure 3. (a) Functionalization of exfoliated flakes of **2** with CNAB. (b) Raman spectroscopy characterization of exfoliated flakes of **2** functionalized with CNAB supported on Si/SiO_2. Control spectra are included.

https://doi.org/10.1021/jacs.1c12072
J. Am. Chem. Soc. 2022, 144, 1119−1124

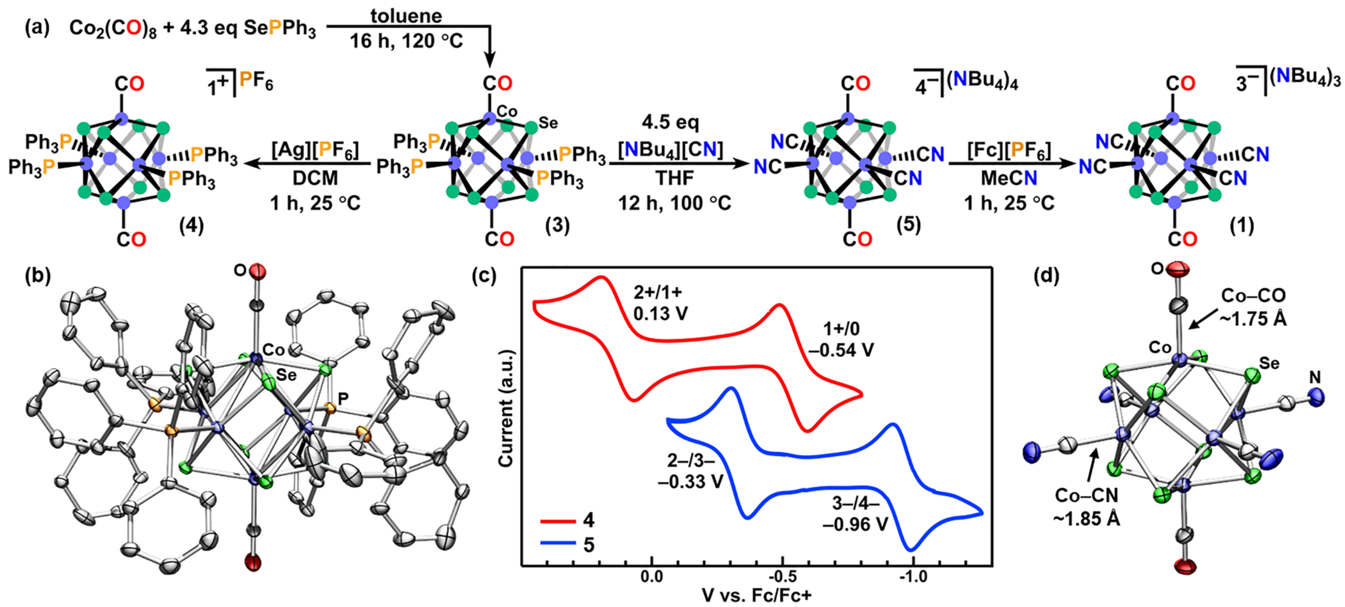

Figure 4. (a) Synthesis of **1** and **3**−**5**. (b) Crystal structure of [*trans*-$Co_6Se_8(PPh_3)_4(CO)_2$][PF_6] (**4**). (c) Cyclic voltammogram of **4** (red) and **5** (blue). (d) Crystal structure of $[NBu_4]_4$[*trans*-$Co_6Se_8(CN)_4(CO)_2$] (**5**). The structures in (b) and (d) are presented with ellipsoids at 30% and 50% probability, respectively. H atoms, solvent molecules, and counterions are omitted for clarity.

solution of CNAB in toluene. The flakes are irradiated with blue light (456 nm) for 4.5 h at room temperature (Figure 3a). The Raman spectrum of exfoliated **2** (before functionalization) shows only a strong CN stretch at 2100 cm^{-1} (Figure 3b, red). After photoinduced surface functionalization, the Raman spectrum of the same exfoliated flake (rinsed with toluene to remove leftover CNAB) shows several Raman peaks between 1400 and 1600 cm^{-1} characteristic of CNAB (Figure 3b, purple).

The Raman spectrum of the same substrate measured away from the flake shows no CNAB signal (Figure 3b, green), indicating CNAB is not indiscriminately sticking to the substrate but is associated specifically with the exfoliated flakes. For reference, we include the Raman spectrum of CNAB dropcast on the Si/SiO_2 substrate (Figure 3b, blue). When exfoliated flakes of **2** are treated with CNAB in toluene for 4.5 h in ambient light, the CNAB Raman peaks are extremely weak (Figure 3b, cyan). This suggests a very small amount of CNAB may bind to **2** through thermal substitution for CO on the cluster or for pyridine on the bridging Co site. Within the resolution of AFM, the thickness and shape of the functionalized flakes is unchanged, indicating the reaction only takes place on the exposed surface, as a significant expansion of the interlayer spacing would result from functionalization of all layers (Figure S13). Overall, these results support the conclusion that the functionalization is in fact the photoinduced exchange of CO for CNAB on the surface of exfoliated flakes of **2**.

The facile photoinduced surface substitution reaction described above can be performed at ambient temperature in a short time frame and without disturbing the in-plane bonding of **2**. Based on the wide variety of molecules featuring isocyanides,[47] our surface modification approach could provide access to 2D materials with a diverse set of functional groups. Given the solution phase precedent,[46] we expect this method to also work with other strong ligands such as alkyl phosphines, further expanding the scope of surface functionalities.

The regioselective synthesis of the 2D superatomic node is a critical step in the rational assembly of the versatile 2D material described above (Figure 4a). We first prepare site-differentiated *trans*-$Co_6Se_8(PPh_3)_4(CO)_2$ (**3**) by heating to reflux a solution of $Co_2(CO)_8$ with 4.3 equiv of $SePPh_3$ in toluene.[44] A suspension is obtained after 12 h, which is filtered hot to give **3** in 97% yield. This reaction can be run on a multigram scale, and the *trans* cluster is the sole product, obviating the need for any subsequent purification. The IR spectrum of **3** shows a single CO stretch (Figure S14), and the ^1H and ^{31}P nuclear magnetic resonance (NMR) spectra confirm the presence of one symmetry-distinct PPh_3 site. Although **3** is insoluble in most solvents at room temperature, we were able to grow crystals from hot dichloromethane (DCM). SCXRD reveals the *trans* isomer (Figure S1), with two unique cluster halves in the asymmetric unit. To confirm that the insoluble solid obtained from the reaction solely contains **3**, we treated the powder with silver hexafluorophosphate ([Ag][PF_6]) in DCM to exclusively form the soluble, oxidized cluster [*trans*-$Co_6Se_8(PPh_3)_4(CO)_2$][PF_6] (**4**), as determined by IR spectroscopy, NMR, and SCXRD (Figure 4b and Figure S14). Cyclic voltammetry (CV) of **4** in DCM shows two reversible redox events: a reduction to **3** at −0.54 V and an oxidation at 0.13 V vs ferrocene/ferrocenium (Fc/Fc^+, Figure 4c).

The synthesis of the 2D tetracyano superatomic node **1** is as straightforward as that of precursor **3**. The thermally labile PPh_3 ligands allow us to install cyanide ligands via thermal substitution,[48,49] while the CO ligands are kinetically inert under these conditions. Treatment of **3** with 4.5 equiv of tetrabutylammonium cyanide ([NBu_4][CN]) in tetrahydrofuran (THF) at 100 °C for 12 h in a sealed high-pressure reaction vessel gives $[NBu_4]_4$[*trans*-$Co_6Se_8(CN)_4(CO)_2$] (**5**) in 93% yield as a green-brown powder isolated by filtration. The *trans* geometry is determined by analyzing the Co−CN and Co−CO bond metrics from SCXRD of crystals grown from DCM (Figure 4d) and by IR spectroscopy (CO: 1940 cm^{-1}; CN: 2060 cm^{-1}). The crystal structure contains an intact Co_6Se_8

https://doi.org/10.1021/jacs.1c12072
J. Am. Chem. Soc. 2022, 144, 1119−1124

core, and there is no disorder of the CO or CN positions, showing the fidelity of the *trans*-CO positions even at elevated temperature. The CV of **5** shows two reversible oxidations (Figure 4c) with the accessible charge states corresponding to the same three oxidation states of the Co_6Se_8 core seen in the CV of **5**: neutral, 1^+, and 2^+. Each event is cathodically shifted compared to those in **4** due to the tetraanionic nature of **5**. While **5** is air-sensitive in DCM solution, oxidation with ferrocenium hexafluorophosphate yields bench-stable $[NBu_4]_3[trans\text{-}Co_6Se_8(CN)_4(CO)_2]$ (**1**). Oxidation of **5** to **1** shifts the CO and CN stretching frequencies to higher wavenumbers: 1978 cm^{-1} (CO) and 2089 cm^{-1} (CN), consistent with a decrease in backbonding from the less electron-rich core. The final step is to prepare a water-soluble form of **1** via cation metathesis by treating the cluster with sodium tetraphenylborate in acetonitrile. We formulate the brown powder that precipitates from this reaction as "$[Na]_3[trans\text{-}Co_6Se_8(CN)_4(CO)_2]$", though a mixture of sodium and tetrabutylammonium counterions is also possible. The precipitate was used directly in the synthesis of **2**. Overall, this synthesis constitutes a simple, three-step route to an air- and moisture-stable 2D superatomic node.

By designing a site-differentiated superatom with orthogonal chemistry, we have created a vdW superatomic framework that can be exfoliated to produce 2D materials with addressable surfaces. The functionalization of these materials with CNAB serves as proof of concept of the facile replacement of CO ligands on the 2D framework's surface with strong ligands. The ability to decorate the square lattice of **2** with diverse functional groups bound via isocyanides presents unique opportunities for the controlled assembly of heterostructures and even for the surface-templated growth of new materials. Ongoing work using this approach aims to both capitalize on the unique surface chemistry of **2** and to expand the family of 2D superatomic frameworks to include exfoliatable magnetic materials.

■ ASSOCIATED CONTENT

Supporting Information

The Supporting Information is available free of charge at https://pubs.acs.org/doi/10.1021/jacs.1c12072.

Experimental methods, magnetic data, scanning electron microscopy, energy dispersive X-ray spectroscopy, infrared spectra, and crystallographic tables (PDF)

Accession Codes

CCDC 2104724–2104728 contain the supplementary crystallographic data for this paper. These data can be obtained free of charge via www.ccdc.cam.ac.uk/data_request/cif, or by emailing data_request@ccdc.cam.ac.uk, or by contacting The Cambridge Crystallographic Data Centre, 12 Union Road, Cambridge CB2 1EZ, UK; fax: +44 1223 336033.

■ AUTHOR INFORMATION

Corresponding Author

Xavier Roy − *Department of Chemistry, Columbia University, New York, New York 10027, United States*; orcid.org/0000-0002-8850-0725; Email: xr2114@columbia.edu

Authors

Amymarie K. Bartholomew − *Department of Chemistry, Columbia University, New York, New York 10027, United States*

Elena Meirzadeh − *Department of Chemistry, Columbia University, New York, New York 10027, United States*

Ilana B. Stone − *Department of Chemistry, Columbia University, New York, New York 10027, United States*

Christie S. Koay − *Department of Chemistry, Columbia University, New York, New York 10027, United States*

Colin Nuckolls − *Department of Chemistry, Columbia University, New York, New York 10027, United States*; orcid.org/0000-0002-0384-5493

Michael L. Steigerwald − *Department of Chemistry, Columbia University, New York, New York 10027, United States*

Andrew C. Crowther − *Department of Chemistry, Barnard College, New York, New York 10027, United States*

Complete contact information is available at: https://pubs.acs.org/10.1021/jacs.1c12072

Notes

The authors declare no competing financial interest.

■ ACKNOWLEDGMENTS

This work was primarily supported by the NSF CAREER Award DMR-1751949 and the NSF MRSEC on Precision-Assembled Quantum Materials (DMR-2011738). Work on azobenzene ligands was also supported by the NSF CBET (CBET-2017198). A.K.B. was supported by the Arnold O. Beckman Postdoctoral Fellowship in Chemical Sciences. Raman measurements were supported by the Barnard College Provost Office. X-ray diffraction and AFM measurements were performed in the Shared Materials Characterization Laboratory at Columbia University. We are grateful to Columbia University for the support of this facility and to Dr. Manju Rajeswaran for help with instrumentation contained therein. The authors thank Evan J. Telford and Carmela Cuomo for helpful discussions and Victoria Posey and Jennifer Han for assistance splitting glass tubes for the synthesis of **2**. We also thank the Dean Lab in the Department of Physics at Columbia University for the use of their optical microscope.

■ REFERENCES

(1) Le, T. H.; Oh, Y.; Kim, H.; Yoon, H. Exfoliation of 2D Materials for Energy and Environmental Applications. *Chemistry* **2020**, *26* (29), 6360−6401.

(2) Geng, D.; Yang, H. Y. Recent Advances in Growth of Novel 2D Materials: Beyond Graphene and Transition Metal Dichalcogenides. *Adv. Mater.* **2018**, *30* (45), No. e1800865.

(3) Zeng, M.; Xiao, Y.; Liu, J.; Yang, K.; Fu, L. Exploring Two-Dimensional Materials toward the Next-Generation Circuits: From Monomer Design to Assembly Control. *Chem. Rev.* **2018**, *118* (13), 6236−6296.

(4) Zhang, J.; Jia, S.; Kholmanov, I.; Dong, L.; Er, D.; Chen, W.; Guo, H.; Jin, Z.; Shenoy, V. B.; Shi, L.; Lou, J. Janus Monolayer Transition-Metal Dichalcogenides. *ACS Nano* **2017**, *11* (8), 8192−8198.

(5) Mitrović, A.; Abellán, G.; Hirsch, A. Covalent and non-covalent chemistry of 2D black phosphorus. *RSC Adv.* **2021**, *11* (42), 26093−26101.

(6) Tofan, D.; Sakazaki, Y.; Walz Mitra, K. L.; Peng, R.; Lee, S.; Li, M.; Velian, A. Surface Modification of Black Phosphorus with Group 13 Lewis Acids for Ambient Protection and Electronic Tuning. *Angew. Chem.* **2021**, *133* (15), 8410−8417.

(7) Ren, X.; Liao, G.; Li, Z.; Qiao, H.; Zhang, Y.; Yu, X.; Wang, B.; Tan, H.; Shi, L.; Qi, X.; Zhang, H. Two-dimensional MOF and COF

nanosheets for next-generation optoelectronic applications. *Coord. Chem. Rev.* **2021**, *435*, 213781.
(8) Solomos, M. A.; Claire, F. J.; Kempa, T. J. 2D molecular crystal lattices: advances in their synthesis, characterization, and application. *J. Mater. Chem. A* **2019**, *7* (41), 23537−23562.
(9) Liu, X.; Hersam, M. C. Interface Characterization and Control of 2D Materials and Heterostructures. *Adv. Mater.* **2018**, *30* (39), No. e1801586.
(10) Somorjai, G. A.; Li, Y. Impact of surface chemistry. *Proc. Natl. Acad. Sci. U. S. A.* **2011**, *108* (3), 917−24.
(11) Guo, Y.; Dai, B.; Peng, J.; Wu, C.; Xie, Y. Electron Transport in Low Dimensional Solids: A Surface Chemistry Perspective. *J. Am. Chem. Soc.* **2019**, *141* (2), 723−732.
(12) Zhong, X.; Lee, K.; Choi, B.; Meggiolaro, D.; Liu, F.; Nuckolls, C.; Pasupathy, A.; De Angelis, F.; Batail, P.; Roy, X.; Zhu, X. Superatomic Two-Dimensional Semiconductor. *Nano Lett.* **2018**, *18* (2), 1483−1488.
(13) Lee, K.; Choi, B.; Plante, I. J.; Paley, M. V.; Zhong, X.; Crowther, A. C.; Owen, J. S.; Zhu, X.; Roy, X. Two-Dimensional Fullerene Assembly from an Exfoliated van der Waals Template. *Angew. Chem., Int. Ed. Engl.* **2018**, *57* (21), 6125−6129.
(14) Champsaur, A. M.; Yu, J.; Roy, X.; Paley, D. W.; Steigerwald, M. L.; Nuckolls, C.; Bejger, C. M. Two-Dimensional Nanosheets from Redox-Active Superatoms. *ACS Cent Sci.* **2017**, *3* (9), 1050−1055.
(15) Choi, B.; Yu, J.; Paley, D. W.; Trinh, M. T.; Paley, M. V.; Karch, J. M.; Crowther, A. C.; Lee, C. H.; Lalancette, R. A.; Zhu, X.; Kim, P.; Steigerwald, M. L.; Nuckolls, C.; Roy, X. van der Waals Solids from Self-Assembled Nanoscale Building Blocks. *Nano Lett.* **2016**, *16* (2), 1445−9.
(16) Turkiewicz, A.; Paley, D. W.; Besara, T.; Elbaz, G.; Pinkard, A.; Siegrist, T.; Roy, X. Assembling hierarchical cluster solids with atomic precision. *J. Am. Chem. Soc.* **2014**, *136* (45), 15873−6.
(17) Wang, Z. Y.; Wang, M. Q.; Li, Y. L.; Luo, P.; Jia, T. T.; Huang, R. W.; Zang, S. Q.; Mak, T. C. W. Atomically Precise Site-Specific Tailoring and Directional Assembly of Superatomic Silver Nanoclusters. *J. Am. Chem. Soc.* **2018**, *140* (3), 1069−1076.
(18) Pinkard, A.; Champsaur, A. M.; Roy, X. Molecular Clusters: Nanoscale Building Blocks for Solid-State Materials. *Acc. Chem. Res.* **2018**, *51* (4), 919−929.
(19) Roy, X.; Lee, C. H.; Crowther, A. C.; Schenck, C. L.; Besara, T.; Lalancette, R. A.; Siegrist, T.; Stephens, P. W.; Brus, L. E.; Kim, P.; Steigerwald, M. L.; Nuckolls, C. Nanoscale atoms in solid-state chemistry. *Science* **2013**, *341* (6142), 157−60.
(20) O'Brien, E. S.; Trinh, M. T.; Kann, R. L.; Chen, J.; Elbaz, G. A.; Masurkar, A.; Atallah, T. L.; Paley, M. V.; Patel, N.; Paley, D. W.; Kymissis, I.; Crowther, A. C.; Millis, A. J.; Reichman, D. R.; Zhu, X. Y.; Roy, X. Single-crystal-to-single-crystal intercalation of a low-bandgap superatomic crystal. *Nat. Chem.* **2017**, *9* (12), 1170−1174.
(21) Choi, B.; Lee, K.; Voevodin, A.; Wang, J.; Steigerwald, M. L.; Batail, P.; Zhu, X.; Roy, X. Two-Dimensional Hierarchical Semiconductor with Addressable Surfaces. *J. Am. Chem. Soc.* **2018**, *140* (30), 9369−9373.
(22) Kephart, J. A.; Romero, C. G.; Tseng, C. C.; Anderton, K. J.; Yankowitz, M.; Kaminsky, W.; Velian, A. Hierarchical nanosheets built from superatomic clusters: properties, exfoliation and single-crystal-to-single-crystal intercalation. *Chem. Sci.* **2020**, *11* (39), 10744−10751.
(23) Shores, M. P.; Beauvais, L. G.; Long, J. R. Cluster-Expanded Prussian Blue Analogues. *J. Am. Chem. Soc.* **1999**, *121* (4), 775−779.
(24) Beauvais, L. G.; Shores, M. P.; Long, J. R. Cyano-Bridged Re6Q8(Q = S, Se) Cluster-Cobalt(II) Framework Materials: Versatile Solid Chemical Sensors. *J. Am. Chem. Soc.* **2000**, *122* (12), 2763−2772.
(25) Bennett, M. V.; Beauvais, L. G.; Shores, M. P.; Long, J. R. Expanded Prussian blue analogues incorporating [Re6Se8(CN)6](3-/4-) clusters: adjusting porosity via charge balance. *J. Am. Chem. Soc.* **2001**, *123* (33), 8022−32.
(26) Naumov, N. G.; Ledneva, A. Y.; Kim, S.-J.; Fedorov, V. E. New trans-[Re6S8(CN)4L2] n- Rhenium Cluster Complexes: Syntheses, Crystal Structures and Properties. *J. Cluster Sci.* **2009**, *20* (1), 225−239.
(27) Kim, Y.; Fedorov, V. E.; Kim, S.-J. Novel compounds based on [Re6Q8(L)6]4- (Q = S, Se, Te; L = CN, OH) and their applications. *J. Mater. Chem.* **2009**, *19* (39), 7178−7190.
(28) Litvinova, Y. M.; Gayfulin, Y. M.; Kovalenko, K. A.; Samsonenko, D. G.; van Leusen, J.; Korolkov, I. V.; Fedin, V. P.; Mironov, Y. V. Multifunctional Metal-Organic Frameworks Based on Redox-Active Rhenium Octahedral Clusters. *Inorg. Chem.* **2018**, *57* (4), 2072−2084.
(29) Zheng, Z.; Tu, X. Crystal engineering supported by the [Re6(μ3-Se)8]2+ core-containing clusters. *CrystEngComm* **2009**, *11* (5), 707−719.
(30) Selby, H. D.; Roland, B. K.; Carducci, M. D.; Zheng, Z. Hydrogen-bonded extended arrays of the [Re6(mu3-Se)8]2+ core-containing clusters. *Inorg. Chem.* **2003**, *42* (5), 1656−62.
(31) Yoon, B.; Luedtke, W. D.; Barnett, R. N.; Gao, J.; Desireddy, A.; Conn, B. E.; Bigioni, T.; Landman, U. Hydrogen-bonded structure and mechanical chiral response of a silver nanoparticle superlattice. *Nat. Mater.* **2014**, *13* (8), 807−11.
(32) Huang, R. W.; Wei, Y. S.; Dong, X. Y.; Wu, X. H.; Du, C. X.; Zang, S. Q.; Mak, T. C. W. Hypersensitive dual-function luminescence switching of a silver-chalcogenolate cluster-based metal-organic framework. *Nat. Chem.* **2017**, *9* (7), 689−697.
(33) Mallah, T.; Thiebaut, S.; Verdaguer, M.; Veillet, P. High-Tc Molecular-Based Magnets: Ferrimagnetic Mixed-Valence Chromium(III)-Chromium(II) Cyanides with Tc at 240 and 190 K. *Science* **1993**, *262* (5139), 1554−7.
(34) Huang, Y.; Ren, S. Multifunctional Prussian blue analogue magnets: Emerging opportunities. *Applied Materials Today* **2021**, *22*, 100886.
(35) Entley, W. R.; Treadway, C. R.; Girolami, G. S. Molecular Magnets Constructed from Cyanometalate Building Blocks. *Molecular Crystals and Liquid Crystals Science and Technology. Section A. Molecular Crystals and Liquid Crystals* **1995**, *273* (1), 153−166.
(36) Yan, B.; Zhou, H.; Lachgar, A. Octahedral niobium chloride clusters as building blocks of templated prussian blue framework analogues. *Inorg. Chem.* **2003**, *42* (26), 8818−22.
(37) Zhang, J.; Lachgar, A. Superexpanded Prussian-blue analogue with [Fe(CN)6]4-, [Nb6Cl12(CN)6]4-, and [Mn(salen)]+ as building units. *J. Am. Chem. Soc.* **2007**, *129* (2), 250−1.
(38) Weeks, C.; Franz, M. Topological insulators on the Lieb and perovskite lattices. *Phys. Rev. B* **2010**, *82* (8), 085310.
(39) Jiang, W.; Huang, H.; Liu, F. A Lieb-like lattice in a covalent-organic framework and its Stoner ferromagnetism. *Nat. Commun.* **2019**, *10* (1), 2207.
(40) Cui, B.; Zheng, X.; Wang, J.; Liu, D.; Xie, S.; Huang, B. Realization of Lieb lattice in covalent-organic frameworks with tunable topology and magnetism. *Nat. Commun.* **2020**, *11* (1), 66.
(41) Jiang, W.; Zhang, S.; Wang, Z.; Liu, F.; Low, T. Topological Band Engineering of Lieb Lattice in Phthalocyanine-Based Metal-Organic Frameworks. *Nano Lett.* **2020**, *20* (3), 1959−1966.
(42) Jin, E.; Asada, M.; Xu, Q.; Dalapati, S.; Addicoat, M. A.; Brady, M. A.; Xu, H.; Nakamura, T.; Heine, T.; Chen, Q.; Jiang, D. Two-dimensional sp(2) carbon-conjugated covalent organic frameworks. *Science* **2017**, *357* (6352), 673−676.
(43) Hayami, S.; Komatsu, Y.; Shimizu, T.; Kamihata, H.; Lee, Y. H. Spin-crossover in cobalt(II) compounds containing terpyridine and its derivatives. *Coord. Chem. Rev.* **2011**, *255* (17−18), 1981−1990.
(44) Champsaur, A. M.; Velian, A.; Paley, D. W.; Choi, B.; Roy, X.; Steigerwald, M. L.; Nuckolls, C. Building Diatomic and Triatomic Superatom Molecules. *Nano Lett.* **2016**, *16* (8), 5273−7.
(45) Gadjieva, N. A.; Champsaur, A. M.; Steigerwald, M. L.; Roy, X.; Nuckolls, C. Dimensional Control of Assembling Metal Chalcogenide Clusters. *Eur. J. Inorg. Chem.* **2020**, *2020* (14), 1245−1254.
(46) Gunasekaran, S.; Reed, D. A.; Paley, D. W.; Bartholomew, A. K.; Venkataraman, L.; Steigerwald, M. L.; Roy, X.; Nuckolls, C. Single-Electron Currents in Designer Single-Cluster Devices. *J. Am. Chem. Soc.* **2020**, *142* (35), 14924−14932.

(47) Bode, M. L.; Gravestock, D.; Rousseau, A. L. Synthesis, Reactions and Uses of Isocyanides in Organic Synthesis. An Update. *Org. Prep. Proced. Int.* **2016**, *48* (2), 89−221.
(48) Beauvais, L. G.; Shores, M. P.; Long, J. R. Cyano-Bridged Re6Q8(Q = S, Se) Cluster-Metal Framework Solids: A New Class of Porous Materials. *Chem. Mater.* **1998**, *10* (12), 3783−3786.
(49) Gray, T. G.; Holm, R. H. Site-differentiated hexanuclear rhenium(III) cyanide clusters [Re(6)Se(8)(PEt(3))(n)()(CN)(6)(−)(n)()](n)()(−)(4) (n = 4, 5) and kinetics of solvate ligand exchange on the cubic [Re(6)Se(8)](2+) Core. *Inorg. Chem.* **2002**, *41* (16), 4211−6.

https://doi.org/10.1021/jacs.1c12072
J. Am. Chem. Soc. 2022, 144, 1119−1124